Contributions to Milky Way – M31 Halo Major Merger Remnant Energy

Eason Wang[1,2]*

[1]*Department of Astronomy/Steward Observatory, University of Arizona, 933 North Cherry Avenue, Tucson, AZ 85721, USA*
[2]*Department of Physics, University of Arizona, 1118 E Fourth Street, Tucson, AZ 85721, USA*

8 May 2025

ABSTRACT

Dark matter, although cannot be seen visually, plays an important role in the formation and evolution of galaxies, and makes up the majority of the matter in the universe. Therefore, studying how dark matter haloes interact through merger simulations is important and will help us understand what roles they play in shaping the galaxies that we see today. In this work, we explored this topic through analyzing the particle simulation of the Milky Way (MW)-M31-M33 system created by van der Marel et al. (2012). Specifically, we studied how the haloes of MW and M31 each contributed to the matter distribution of their merger remnant, as well as how the haloes' respective energies before merger may have given rise to their differences in contribution. We found that through the merger, M31 halo particles fell more inward compared to MW halo particles in the merger. We believe that this is likely due to M31 being more energetic than MW before the merger, and therefore interacting more strongly during collision and losing more energy, causing its particles to fall in more than MW particles. This result sheds some light on what merger histories could give rise to different elliptical galaxies with varying dark matter concentrations near the center.

Key words: Dark Matter Halo – Major Merger – Minor Merger – Hernquist Profile – Virial Radius

1 INTRODUCTION

Dark matter, although yet to be identified, is now considered to be an essential part of the universe, surrounding galaxies in a structure called a **dark matter halo**. The need for a dark matter halo model became apparent in the last century when observational evidence showed that more mass was needed beyond baryonic matter for spiral galaxies to be stable (Ostriker et al. 1974). This, along with the fact that Newtonian gravity fails to explain the observed galactic dynamics, led Willman & Strader (2012) to define a **galaxy** as *a gravitationally bound collection of stars whose properties cannot be explained by a combination of baryons and Newton's laws of gravity*. Over the past decades, advances in computation and simulations have revealed to us ever finer details in halo structure. Among these simulations, galaxy merger simulations are particularly useful for studying how certain galaxies are structured the way they do today, as mergers happen frequently in the universe. For example, **major mergers**, which are mergers of two galaxies with a mass ratio of 4:1 or lower, explains our observations of irregular and starburst galaxies (Renaud et al. 2022).

Dark matter haloes are sites where gravity wins over the expansion force of the universe, so they are where galaxies form. Therefore, studying how halo structure changes through a major merger can help us understand **galaxy evolution**, which is how galaxies form and change over time. Specifically, understanding the structure of individual haloes and how they change through mergers can greatly inform us about the merger history of the galaxies we observe. In our observations, we only see one snapshot of a galaxy, so simulations are a good way for us to study how galaxies evolve and allow us to map

each observed galaxy to a stage in its evolution. This work will be done using an N-body simulation of the Milky Way (MW)-M31-M33 system by van der Marel et al. (2012).

The connection between merger history and the resulting halo structure has been extensively studied. For example, major mergers, as opposed to **minor mergers** (where the mass ratio of haloes is 4:1 or higher), have been found to bring more material to the halo center, allowing for more homogeneous mixing (Frenk & White 2012). Past studies using merger simulations have found major connections between orbital parameters and the resulting halo shape (Drakos et al. 2019a), as well as between the energy of the merger encounter and the final mass distribution (Drakos et al. 2019b). In another simulation study, Abadi et al. (2010) demonstrated that haloes become more axisymmetric through mergers. As shown in Figure 1, Drakos et al. (2019b) also provides the interesting result that the virial mass of the merged halo is not merely the sum of the virial masses of the initial haloes. The virial mass is the mass enclosed within the **virial radius** (r_{vir}), which is strictly defined as the radius within which the virial theorem applies. However, for this work, we will define v_{vir} to be the radius within which the enclosed dark matter density is 360 times that of the universe.

On the matter of halo mergers, further work could be done in exploring a wider variety of mergers, as studies like Drakos et al. (2019a) only explored mergers of identical haloes. After all, the vast majority of mergers in the universe are minor mergers, so they account for the formation of a larger fraction of the galaxies we observe. For instance, minor mergers could help explain the open question left by Drakos et al. (2019b), which is that the central density in haloes seem to drop as they grow in size. With major mergers, however, there is also more interesting physics to be explored. It is still unclear how in major merger simulations, the central concentration
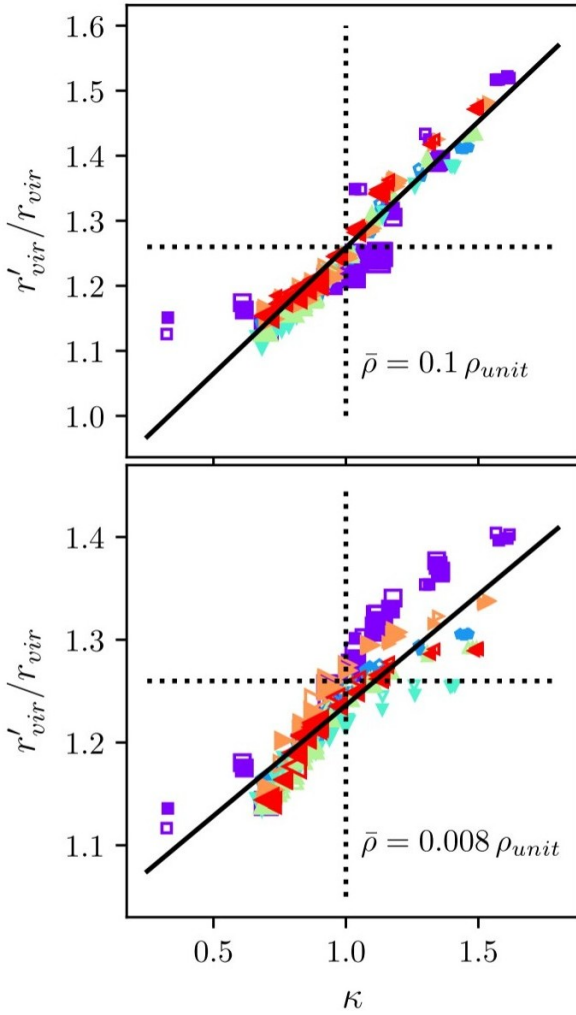
---

* E-mail: wxs0703@arizona.edu

Figure 1. The change in virial radius r'_{vir}/r_{vir} as a function of the relative energy change κ. Virial mass scales as r^3_{vir}, so this figure also shows a wide distribution in mass scaling after merger despite starting with two equal mass haloes. Figure taken from Drakos et al. (2019b). The meanings of the colors and symbols are described in the paper, however they are not relevant to this work.

seems to increase rather than decrease (Drakos et al. 2019b). Another area of study is the contribution of each progenitor halo in the spin, shape, and matter distribution of the merger remnant, which is what we will be exploring in this work. This paper is organized as follows: In Section 2, we motivate the specific question that will be explored. In Section 3, we describe the computational and analysis methods used for this project. In Section 4 we present the results. We discuss the results and conclude in Section 5.

2 THIS PROJECT

In this paper, we will study the contributions of MW and M31 halo particles to the density profile of the merged remnant. It will be interesting to explore the distribution of halo particles from both MW and M31 within the merged remnant to see if either system contributes more in certain regions. Then, we will explore the connections between the different density profile contributions and the energy distributions of each system before and after merger. Following Drakos et al. (2019b), We will also explore how the virial radius

of the halo changes after merger, and explore its relationship with the energy components of the system.

This work will mark as part of the exploration into how each major merger halo contribute to the merged system, as mentioned in Section 1. Specifically, we are exploring the matter distribution of the haloes by computing and comparing density profiles. We will also be exploring the internal energy distributions of the haloes before and after merger to attempt to make a connection between that and the density profile contributions.

Understanding the intricacies of merger contributions is important, as it could allow us to better infer kinematic and merger histories of haloes from observations of their current state. Using the MW-M31-M33 system as a case study, this work will demonstrate how various initial halo properties could cause subtle differences in contribution to the density profile of the merged halo.

3 METHODOLOGY

For this project, we will be using the N-body simulation for the MW-M31-M33 system described in van der Marel et al. (2012). An N-body simulation is a numerical simulation of many particles in a physical system. This simulation models the initial conditions of the system consistent with current measurements, and models each galaxy using three types of particles: halo, disk, and bulge. The distribution of halo particles for each galaxy follows a **Hernquist Profile** (Hernquist 1990), which is a halo profile whose density function $\rho(r)$ has the form

$$\rho(r) = \frac{M}{2\pi} \frac{a}{r(r+a)^3}, \tag{1}$$

where r is the radius from center of halo, M is the total mass of the halo, and a is the scale length which is fitted for each galaxy. The disk and bulge of each galaxy follows exponential profiles, whose parameters follow past literature, and M33 is taken to be bulgeless.

For this study, we will only be using the halo particles in the simulation. We will also be using a few snapshots of the simulation at the highest resolution (HighRes), as we are only comparing before and after merger states, not studying the evolution of the system over time. The initial comparison of density profiles will be made using the first and last snapshots of the simulation (0 and 801). As analysis continues, we might need to use snapshots closer to the merge event (i.e. close to the first pericenter or just after merge completes) to get a better idea of how energy transfers in the system through the merger. The relevant snapshots can be easily identified by plotting the relative positions of MW and M31 over all the snapshots, as shown in Figure 2. The first pericenter is the first local minima in the plot, and we defined the merged state as the snapshot after which the distance between the center of masses of MW and M31 is less than 5 kpc. As the steps for this study depends on the results of the previous step, we show a decision tree in Figure 3 to illustrate the process. This work will be limited to only analyzing density profiles and the energy components of the system.

To find the contributions of MW and M31 halo particles in the density profile of the merged system, we will plot the density profiles of both systems at the last snapshot individually and then over-plot the sum of their profiles for the profile of the merger remnant. To compute the density profile, we will first compute the enclosed mass profile $M_{enc}(r)$ for a set of radial bins R_i, by simply summing the masses of all the particles contained within R_i. After that, the density ρ_j between bins R_i and R_{i+1} can be calculated by
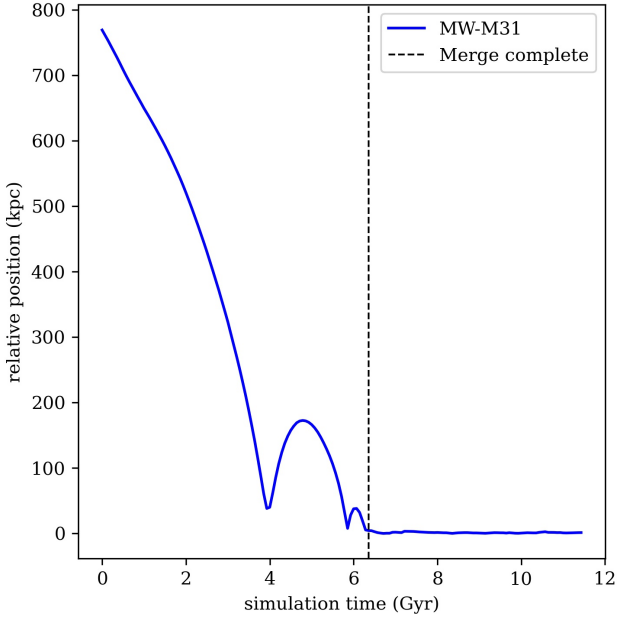
Figure 2. The relative positions of the center of masses of MW and M31 over the course of the simulation. After the black dashed line, the relative position effectively flattens, showing that the two systems have merged.
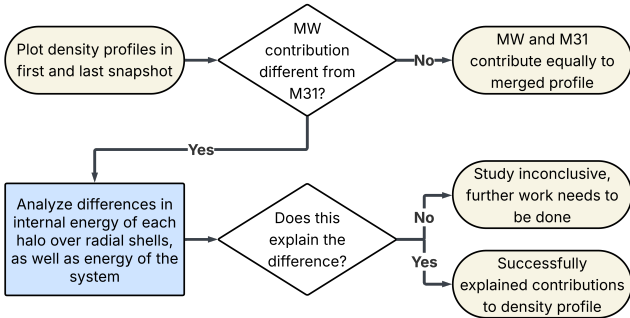

Figure 3. Decision tree illustrating the research process for this work.

$$\rho_j = \frac{M_{enc,i+1} - M_{enc,i}}{V_{enc,i+1} - V_{enc,i}}, \tag{2}$$

where

$$V_{enc,i} = \frac{4}{3}\pi R_i^3. \tag{3}$$

The radii r_j at which the density is ρ_j is then

$$r_i = \frac{R_{i+1} + R_i}{2}. \tag{4}$$

We will plot the density profiles of MW and M31 in the first and last snapshot. Plotting the first snapshot is more as a sanity check, as the initial halo profiles for MW and M31 in this simulation should look the same. We will focus on the profiles in the last snapshot to examine whether either halo's matter dominates more in a certain radial region. If there is a difference in contribution, we will then analyze the energies of each system, where the total energy $E = U + K$,

where U is the total gravitational potential energy of the halo, and K is the total internal kinetic energy of the halo. To calculate U, we need to first fit each profile to a Hernquist profile, following Equation 1. For simplicity, we will use the curvefit function in the SciPy Python package to fit the profile. The gravitational potential energy can be derived by the integral

$$U(r) = -\int_0^r \rho(r)\Phi(r)(4\pi r^2)dr, \tag{5}$$

where $\rho(r)$ is the fitted Hernquist profile, and $\Phi(r)$ is the Hernquist potential given by

$$\Phi(r) = -\frac{GM}{r+a}, \tag{6}$$

where G is the gravitational constant. Evaluating the integral then gives us

$$U(r) = -\frac{GM^2}{6a} + \frac{GM^2 a}{2(r+a)^2} - \frac{GM^2 a^2}{3(r+a)^3}. \tag{7}$$

Now this formula can only be used for computing the potential energy for the entire halo. After the merger, we would also like to find the potential energy components from MW and M31 within the merger. We can derive the formula for that by simply replacing the $\rho(r)$ in Equation 5 with the component's density profile $\rho_i(r)$. Evaluating this integral by hand is however very tedious, so in this work we resort to numerical integration instead. In comparison, the calculation for K is more brute force, where we simply need to calculate the velocity v of each particle relative to the center of mass of the halo, and the internal kinetic energy is then

$$K = \frac{1}{2}\sum_{i=1}^N m_i v_i^2, \tag{8}$$

where m_i is the mass of the ith particle. We will perform this analysis on both the before and after merger snapshots for both MW and M31, as well as the final merger remnant. If there is a difference in contribution, then according to Drakos et al. (2019b), the halo with more energy should contribute more matter in the inner region of the merged halo.

Knowing that the halo particles of M31 has slightly higher rotational velocities, we expect its halo to be more energetic, and therefore contribute more to the inner regions of the merger remnant. Knowing the energies of MW, M31, and the merger remnant, we can also calculate the energy change κ as defined in Drakos et al. (2019b), compute each halo's virial radius, and place the data point on the plot in Figure 1. My data point should align somewhat closely with the other ones.

4 RESULTS

Upon computing the density profiles of MW and M31 at snapshots 0 and 800 of the simulation, we compared their fractional difference of density at both of these snapshots, which we define as

$$f_\rho = \frac{\rho_{M31} - \rho_{MW}}{\rho_{MW}}. \tag{9}$$

The results are plotted in Figure 4. Note that even after merger, the particles of the simulation are clearly separated as MW and M31
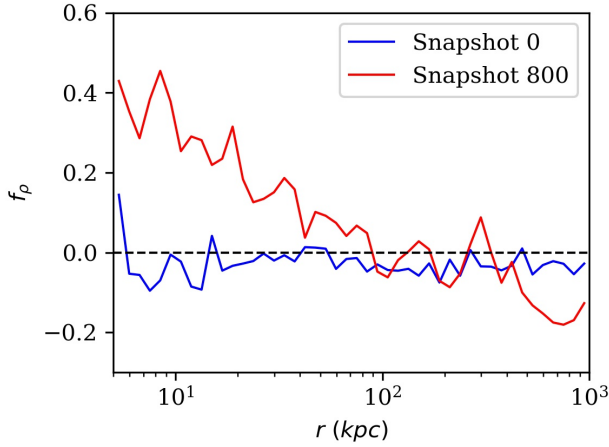
Figure 4. The fractional density difference between M31 and MW at snapshots 0 and 800. Area shaded in grey indicates high uncertainty and should be ignored. This shows that after merger, M31 halo particles moved more inward compared to MW.

Figure 5. The total internal energy of MW and M31 halo particles before and after merger, shown in the top and bottom panels respectively. Note the different y-axis scalings.

particles, so we are able to use that to make the same density profile calculations at snapshot 800. The plot shows that MW and M31 start off with roughly the same profile, as the fractional difference hovers around zero for all radii. After merger, we see a significantly higher matter contribution from M31 to the inner regions of the merger remnant, while MW starts to contribute more after $\sim 500\ kpc$. This prompted an analysis of the internal energy of each system in order to explain this difference in contribution.

Following Equations 7 and 8, we computed the total energy E of MW and M31 particles before and after merger, shown in Figure 5. The top plot shows that M31 overall has a higher internal energy than MW before the merger. After the merger, M31 still has a higher energy, but the distribution moved closer to that of MW. Note that both systems lost energy over the course of the merger. This means that M31 halo particles lost more energy through the merger, which is consistent with our comparison of the density profiles, as particles move inward when there's less energy.

5 DISCUSSION

From our analysis of the internal energies of MW and M31 before and after merger, we have found that the change in the energy distribution is consistent with our observation that M31 particles reside more in the inner region of the merger remnant. This result matches our hypothesis made in Section 3. While not explored in this paper, we can discuss why the internal energy of M31 halo particles decreased more than MW from the merger. Since dynamical friction tends to slow down and draw in the more strongly interacting halo in a major merger (Chandrasekhar 1943; Barnes & Hernquist 1992), we can reasonably guess that the significantly higher internal energy in M31 before merger caused it to be dampened more than MW.

Our results are consistent with Drakos et al. (2019a) in that energetic mergers increase the concentration near the center of the merger remnant. We were also able to highlight this effect as a result of one of the progenitor haloes being more energetic before the merger. Exploring the contributions of progenitor haloes to merger remnants is useful for understanding the subtle differences in the elliptical galaxies we see today. For example, our result suggests that mergers with
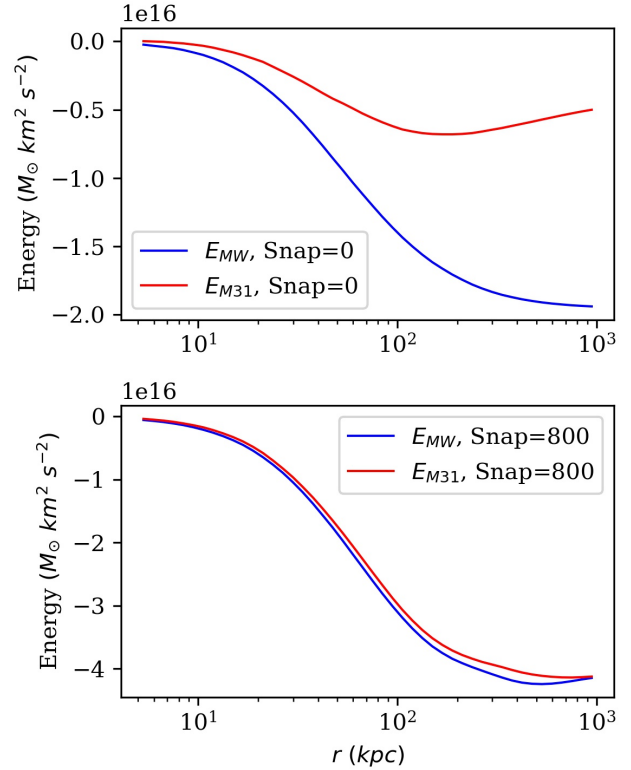
energetic progenitor haloes could have especially high dark matter fraction near the center, which can be indirectly observed through gravitational lensing. Exploring the cause of these phenomena will help us get a clearer picture of how galaxies in our universe evolve overall.

While our results made a connection between the energy distribution changes from the merger and the density profile contributions, we have not clearly identified the exact mechanism through which they are connected. This study could also be improved by analyzing various snapshots close to or during the collision between MW and M31, to check that there is indeed a smooth and traceable trend of M31 particles moving inward and MW particles moving out. We leave the aforementioned extensions to our study for future work.

6 CONCLUSION

We know that dark matter plays an important role in the formation and evolution of galaxies, mostly due to it making up most of the matter of the universe. Therefore, studying how dark matter haloes interact through merger simulations is important and will help us understand what roles they play in shaping the galaxies that we see today. In this work, we explored this topic through analyzing the particle simulation of the Milky Way (MW)-M31-M33 system created by van der Marel et al. (2012). Specifically, we studied how the haloes of MW and M31 each contributed to the matter distribution of their merger remnant, as well as how the haloes' respective energies before merger may have given rise to their differences in contribution.

In this study, we found that through the merger between MW and M31, M31 halo particles fell more inward compared to MW halo particles in the merger. Through our energy analysis of M31 and MW haloes before merger and the merger remnant, we found that M31 started with more internal energy, but converged to around the same level of energy as MW particles after merger. We believe that this fact led to M31 interacting more strongly during collision and losing more energy, causing its particles to move more towards the center of the merger compared to MW particles. This result agrees with our hypothesis made in section 3, and also agrees with the results of previous work (Drakos et al. 2019b).

Moving forward, we would like to look into more detail what was happening to the halo particles during the merger event, and show precisely how the particles are moving on a statistical level over time. This could also be contrasted with an analysis of the internal energies of the systems over time, showing that the changes in matter distribution does indeed correlate with the changes in energy. If computation limits permit, it would also be helpful to explore many realizations of the simulation with slightly different initial conditions, such as small changes in mass distribution and initial trajectories, and see if they make notable differences in the merger remnant. Last but not least, despite dark matter haloes making up most of the mass of galaxies, the baryons in a galaxy has unique physics that could alter the evolution of the entire galaxy as well, so we would also like to include that analysis in a more detailed study.

7 ACKNOWLEDGEMENTS

REFERENCES

Abadi M. G., Navarro J. F., Fardal M., Babul A., Steinmetz M., 2010, Monthly Notices of the Royal Astronomical Society, 407, 435
Astropy Collaboration et al., 2013, A&A, 558, A33
Astropy Collaboration et al., 2018, AJ, 156, 123
Astropy Collaboration et al., 2022, ApJ, 935, 167
Barnes J. E., Hernquist L., 1992, ARA&A, 30, 705
Chandrasekhar S., 1943, ApJ, 97, 255
Diemer B., 2018, ApJS, 239, 35
Drakos N. E., Taylor J. E., Berrouet A., Robotham A. S. G., Power C., 2019a, MNRAS, 487, 993
Drakos N. E., Taylor J. E., Berrouet A., Robotham A. S. G., Power C., 2019b, MNRAS, 487, 1008
Frenk C., White S., 2012, Annalen der Physik, 524, 507
Gommers R., et al., 2025, scipy/scipy: SciPy 1.15.2, doi:10.5281/zenodo.14880408, https://doi.org/10.5281/zenodo.14880408
Harris C. R., et al., 2020, Nature, 585, 357
Hernquist L., 1990, ApJ, 356, 359
Hunter J. D., 2007, Computing in Science & Engineering, 9, 90
Kluyver T., et al., 2016, in Loizides F., Schmidt B., eds, Positioning and Power in Academic Publishing: Players, Agents and Agendas. pp 87 – 90
Ostriker J. P., Peebles P. J. E., Yahil A., 1974, ApJ, 193, L1
Perez F., Granger B. E., 2007, Computing in Science and Engineering, 9, 21
Renaud F., Segovia Otero , Agertz O., 2022, Monthly Notices of the Royal Astronomical Society, 516, 4922
Van Rossum G., Drake F. L., 2009, Python 3 Reference Manual. CreateSpace, Scotts Valley, CA
Virtanen P., et al., 2020, Nature Methods, 17, 261
Wagg T., Broekgaarden F. S., 2024, arXiv e-prints, p. arXiv:2406.04405
Wagg T., Broekgaarden F., Gültekin K., 2024, TomWagg/software-citation-station: v1.2, doi:10.5281/zenodo.13225824, https://doi.org/10.5281/zenodo.13225824
Willman B., Strader J., 2012, The Astronomical Journal, 144, 76
van der Marel R. P., Besla G., Cox T. J., Sohn S. T., Anderson J., 2012, ApJ, 753, 9

This paper has been typeset from a TeX/LaTeX file prepared by the author.